Flavor Structure of the Cosmic-Ray Electron/Positron Excesses at DAMPE

SHAO-FENG GE [a,b] and HONG-JIAN HE [c,d,e]

[a] Kavli IPMU (WPI), UTIAS, The University of Tokyo, Kashiwa, Chiba 277-8583, Japan.
[b] Department of Physics, University of California, Berkeley, CA 94720, USA.
[c] T. D. Lee Institute, Shanghai 200240, China;
School of Physics and Astronomy, Shanghai Jiao Tong University, Shanghai 200240, China.
[d] Institute of Modern Physics, Tsinghua University, Beijing 100084, China.
[e] Center for High Energy Physics, Peking University, Beijing 100871, China.

The Dark Matter Particle Explorer (DAMPE) satellite detector newly announced its first result for measuring the cosmic-ray electron/positron (CRE) energy spectrum up to 4.6 TeV, including a peak-like event excess around 1.4 TeV. We observe a sizable hidden excess in the DAMPE CRE spectrum over a fairly wide region $(0.6 − 1.1)$TeV, which has a non-peak-like structure. We find that this new excess can be explained by a set of 1.4 TeV $\mu^{\pm}$ events with subsequent decays into $e^{\pm}$ plus neutrinos. To explain this new excess together with the 1.4 TeV peak, we show that the *flavor structure* of the original lepton final-state produced by the dark matter (DM) annihilations (or other mechanism) should have a composition ratio $N_e : (N_\mu + \frac{1}{6} N_\tau) \approx 1 : 12.7$. We point out some simple realizations, including the simplest case, $N_e : N_\mu : N_\tau \approx 1 : 12.7 : 0$. We further discuss the implications for the flavor-related DM model buildings. [IPMU17-0173]

1. Introduction

Measuring high energy cosmic ray electrons and positrons (CRE) is important for probing the nearby galactic sources [1] and the possible observation of dark matter (DM) annihilations [2]. The cosmic ray electron/positron spectrum has been probed up to TeV energy scales by the ground-based and space-borne experiments such as HESS [3], VERITAS [4], FermiLAT [6], AMS-02 [5], and CALET [7]. These provide important means for the indirect DM detections.

The Dark Matter Particle Explorer (DAMPE) satellite detector [8] was launched at the end of 2015 and is optimized for measuring cosmic $e^{\pm}$ rays and γ-rays up to about 10 TeV energy. After 530 days of data-taking, the DAMPE collaboration newly announced [9] its first result of detecting the cosmic-ray electron/positron energy spectrum from 25 GeV up to 4.6 TeV. The main part of this spectrum can be fitted by a smoothly borken power-law model and shows a spectral break around 0.9 TeV, which confirms the similar evidence found by HESS [3]. The DAMPE CRE spectrum also indicates a tentative peak-like event excess around 1.4 TeV. This excess has triggered wide interests and attempts to the possible physics implications [10]-[14], either from the conventional astrophysical sources (such as pulsars and supernova remnants) or from dark matter annihilation into $e^{+}e^{-}$ events, as well as building various lepton-related DM models [15].

In this work, we observe sizable new excess over a fairly wide region $(0.6 − 1.1)$TeV on the left-hand-side of the 1.4TeV peak. We attempt to explain this intriguing new excess by considering a set of 1.4TeV $\mu^{\pm}$ events which are produced together with the 1.4TeV $e^{\pm}$ peak events and subsequently decay into $e^{\pm}$ plus neutrinos. For a possible 1.4TeV τ component in the original CRE source, its leading decay contribution to the DAMPE detection is much smaller than muon, but has a similar energy distribution. To explain this new excess together with the 1.4TeV peak, we will show that the *flavor structure* of the original lepton final-state produced by the DM annihilations (or other mechanism) should have a composition ratio $N_e : (N_\mu + \frac{1}{6} N_\tau) \approx 1 : 12.7$.

This paper is organized as follows. In Sec. 2, we first inspect the DAMPE CRE spectrum and point out the additional new event excess over the $(0.6 − 1.1)$TeV region. Then, excluding the data points of this new excess and the 1.4TeV peak, we fit the pure CRE background data points by using the double-broken power-law formula and obtain a rather smooth background curve. In Sec. 3, we will study the decays of 1.4TeV $\mu^{\pm}$ events into $e^{\pm}$ plus neutrinos, which are produced at the same time as the 1.4TeV $e^{\pm}$ peak events. We show that the decay contributions of the 1.4TeV $\mu^{\pm}$ events to the DAMPE CRE spectrum can explain very well the new excess over the $(0.6−1.1)$TeV region. In Sec. 4, we further perform a fit to include the 1.4TeV $e^{\pm}$ events produced in a nearby clump or subhalo source together with the decay contribution of the 1.4TeV $\mu^{\pm}$ events. We also discuss the physics implications for the original flavor structure of the CRE spectrum as detected by DAMPE. Finally, we conclude in Sec. 5.

2. Backgrounds and New Excess Off the Peak

We replot all the DAMPE data points with $\pm 1\sigma$ errors [9] in Fig. 1. This is much clearer since the original plot (Fig.2) of DAMPE [9] also displayed HESS and Fermi-LAT results (for comparison) which have significant overlap with the DAMPE data points around $(0.35 - 2)$TeV region and make the precise feature of DAMPE points less clear in this region.

The DAMPE data points presented in the current Fig. 1 appear distinctive. From this, we observe that the DAMPE data points exhibit another rather interesting structure on the left-hand-side of the 1.4TeV peak. The energy region of $(0.616-1.07)$TeV contains five data points (marked in red color), which all lie above the expected positions (based on the rest of the background points). The five red data points are distinctive and form a new excess in addition to the 1.4TeV peak (marked in blue). In particular, we compare these five red points with the rest and find clear jumps to their neighbouring points (marked in black color) by $\gtrsim 2\sigma$ deviations.

To make this feature fully clear, we first fit the pure background bins (marked by black color in the current Fig. 1), without including the five red data points around $(0.616 - 1.07)$TeV and the blue peak point at 1.4TeV. For this pure background fit, we use the double-broken power-law form [16],

$$\Phi_{\rm bkg} = \frac{\Phi_0}{E_e^\gamma}\left[1+\left(\frac{E_{\rm br,1}}{E_e}\right)^\delta\right]^{\frac{\Delta\gamma_1}{\delta}}\left[1+\left(\frac{E_e}{E_{\rm br,1}}\right)^\delta\right]^{\frac{\Delta\gamma_2}{\delta}}. \quad (1)$$

According to the recent results of Fermi-LAT [6] and DAMPE [9], we can set the first break $E_{\rm br,1} = 50\,{\rm GeV}$ and the sharpness parameter $\delta = 10$.

Then, we perform a minimal χ^2 fit

$$\chi^2 = \sum_j \left[\frac{E_e^3\Phi_e(E_j) - \mathcal{O}_j}{\Delta\mathcal{O}_j}\right]^2, \quad (2)$$

for all the background data points (black color) shown in Fig. 1. In Eq.(2), each experimental central value and its error are expressed as $\mathcal{O}_j$ and $\Delta\mathcal{O}_j$, respectively. Our fit gives: $\Phi_0 = 244\,{\rm GeV}^{-1}$, $\gamma = 3.1$, $E_{\rm br,2} = 493\,{\rm GeV}$, and $(\Delta\gamma_1, \Delta\gamma_2) = (0.1, -0.57)$.

We plot our fit of the pure background contributions by the black curve in Fig. 1. This new background curve is fairly smooth and has better quality. It shows that above these backgrounds, the DAMPE data exhibit two distinctive structures of excesses: (i) one is the previously noticed 1.4 TeV peak excess ($\gtrsim 3\sigma$) marked by the
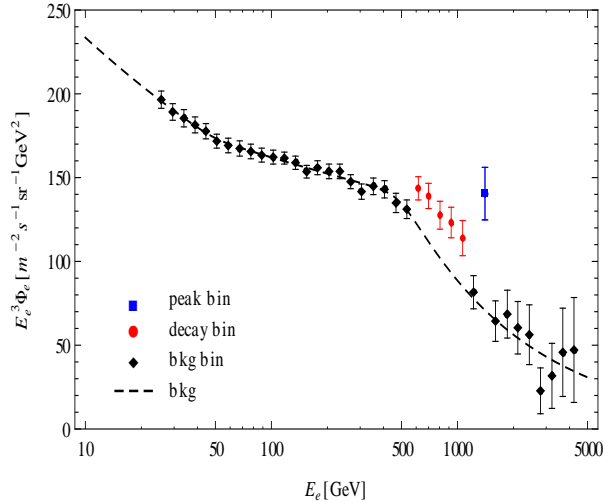

FIG. 1. Fitting the pure background CRE spectrum (black data points) at DAMPE, as shown by the black curve. The blue peak point (around 1.4TeV) is more than 3σ above the black curve and the 5 red data points in the $(0.6 - 1.1)$TeV region are more than 2σ above the black curve, so they are not included in this pure background fitting (black curve).

blue point; and (ii) another is the new excess ($\gtrsim 2\sigma$) in the $(0.616 - 1.07)$ TeV region. Although this non-peak type excess is at 2σ level and far from definitive, it is rather suggestive and intrigues us to speculate that this excess may be interconnected with the 1.4TeV peak. We further note that the vertical axis of Fig. 1 is weighted by the cubic energy factor E_e^3 and the actual event numbers of the excess in the 5 bins of the $(0.616-1.07)$TeV region are much larger than that in the 1.4TeV peak bin (with significantly higher energy). In the next section, we shall propose a possible origin for this intriguing non-peak-like structure nearby the 1.4TeV peak.

3. Decays of Muon Composition for New Excess

Inspecting the non-peak-like new excess over the $(0.616 - 1.07)$TeV region of Fig. 1, we conjecture that it originates from the decays of 1.4TeV muons. These muon events were produced at the same time when the 1.4TeV $e^\pm$ events were generated, say, during the DM annihilations in a nearby clump or subhalo. Once $\mu^\pm$ events are produced, they will decay predominantly into $e^\pm$ via the 3-body channel with almost 100% branching fraction [17], $\mu \to e\bar{\nu}_e\nu_\mu$. A flying muon with 1.4TeV energy has a lifetime about 0.026s and could only travel about 7.8×10^6m. This distance is negligible when compared to the nearby potential DM sources (typically within ~ 1kpc distance from the earth [10]). All the $\mu^\pm$
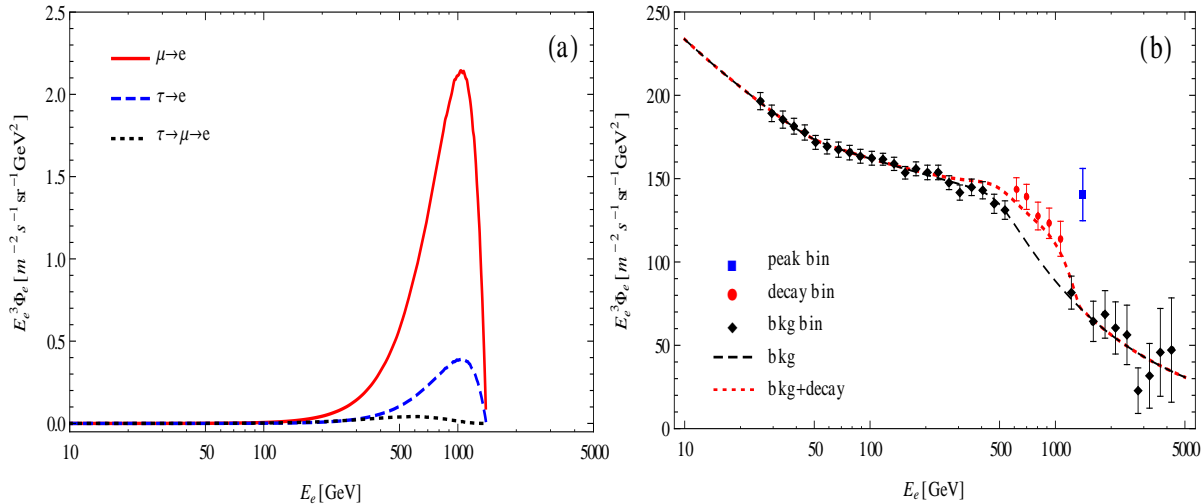
FIG. 2. Plot-(a): Electron energy spectrum from the decays of 1.4 TeV muon and tau. The red curve depicts the electron energy distribution from muon decay $\mu \to e\,\bar{\nu}_e \nu_\mu$; the blue curve shows the electron energy distribution from tau decay $\tau \to e\,\bar{\nu}_e \nu_\tau$; and the black curve presents the electron energy distribution from the decay-chain of tau $\tau \to \mu\,\bar{\nu}_\mu \nu_\tau \to e\,\bar{\nu}_e \nu_\mu \bar{\nu}_\mu \nu_\tau$. Plot-(b): Fitting the background spectrum (black data points) together with the non-peak excess (red data points) by including decays of the 1.4 TeV $\mu^\mp$ composition, shown by the red curve.

events would convert into $e^\pm$ events, long before they possibly reach the DAMPE detector.

The $e^\pm$ flux from muon decay is given by $\Phi_{\mu \to e} = N_\mu \frac{1}{\Gamma} \frac{d\Gamma}{dE_e}$, as a product of the muon event number N_μ and the normalized $e^\pm$ spectrum, which we compute as follows,

$$\frac{1}{\Gamma}\frac{d\Gamma}{dE_e} \simeq \frac{4}{E_\mu}\left(\frac{5}{12} - \frac{3E_e^2}{4E_\mu^2} + \frac{E_e^3}{3E_\mu^3}\right), \qquad (3)$$

for $E_e, E_\mu \gg m_e, m_\mu$. The E_e^3 weighted $e^\pm$ energy spectrum is shown as the red solid curve in Fig. 2(a). The major contribution to $E_e^3 \Phi_e$ appears around $(0.6-1.1)$TeV which fully match the new excess region we identified in Sec. 2. The final-state $e^\pm$ from 1.4 TeV muon decays are really promising to explain this new excess.

The $\tau^\pm$ lepton can decay into $e^\pm$ via two channels, the single 3-body-decay $\tau \to e\,\bar{\nu}_e \nu_\tau$ and the chain decay $\tau \to \mu\bar{\nu}_\mu \nu_\tau \to (e\,\bar{\nu}_e \nu_\mu)\bar{\nu}_\mu \nu_\tau$. Since each decay process is mediated by the same $W^\pm$ bosons with exactly the same gauge coupling and the lepton masses are negligible as compared to the large initial lepton-energy (1.4 TeV), the decay $\tau \to e\,\bar{\nu}_e \nu_\tau$ shares almost the same $e^\pm$ spectrum from the muon decay. The major difference comes from their decay branching fractions [17], $\mathrm{Br}[\mu \to e\,\bar{\nu}_e \nu_\mu] \simeq 100\%$ and $\mathrm{Br}[\tau \to e\,\bar{\nu}_e \nu_\tau] \simeq 17.83\% \simeq 1/5.6$. In Fig. 2(a), we present the $e^\pm$ spectrum from the 3-body-decays of muon by the solid red curve and that of tau by the dashed blue curve. Also, the decay $\tau \to \mu\,\bar{\nu}_\mu \nu_\tau$

has a branching fraction 17.4%. For the chain decay, the $e^\pm$ comes from the secondary decay product $\mu^\pm$ and thus has much lower energy. Consequently, its contribution to $E_e^3 \Phi_e$ is highly suppressed, shown by the dotted black curve in Fig. 2(a). Hence, the major contribution of tau decay comes from $\tau \to e\,\bar{\nu}_e \nu_\tau$, which has a similar electron energy distribution to that of the muon decay, but with a suppression factor $\sim \frac{1}{6}$. This means that the decay contributions of muon and tau to the DAMPE CRE spectrum are highly degenerate. For the given (μ, τ) event numbers (N_μ, N_τ), their total contribution is equivalent to $(N_\mu + \frac{1}{6}N_\tau)$ number of muon decay events. So the decay contribution of a possible tau component to the CRE spectrum is minor. The simplest realization is that all decay contributions arise from the muon events.

For comparison, in Fig. 2(a) we set the number of muon and tau events be the same as the peak electron events. Although the peak data in Fig. 1 is much higher than the background curve (with a difference around 70 for $E_e^3 \Phi_e$), the decay spectrum is much lower. The difference comes from the fact that the peak bin is around 1.4 TeV, but the decay peak is around 1 TeV. The weight factor E_e^3 can lead to an enhancement factor $1.4^3 \sim 2.7$ in the plot. Furthermore, the electron excess around 1.4 TeV is distributed within a single bin, while the decay spectrum spreads a much wider region of $(0.616 - 1.07)$TeV. Providing the new excess in this region requires much more muon events
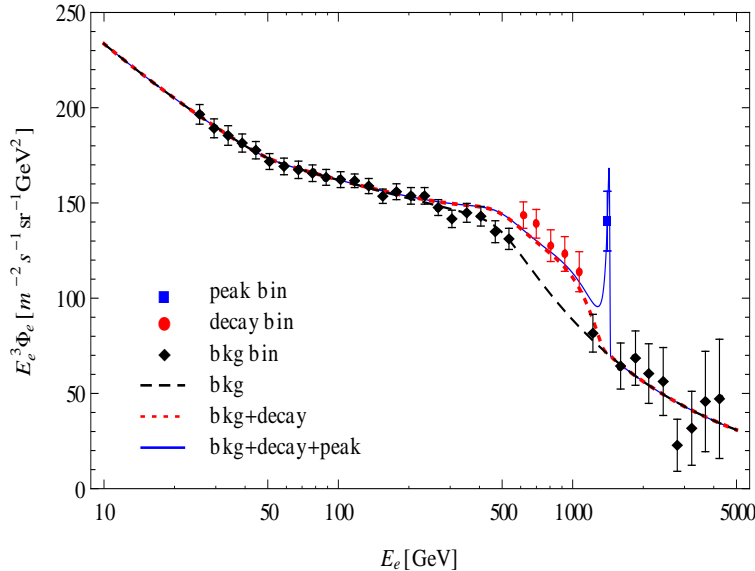
FIG. 3. CRE spectrum for DAMPE: including both the decay contributions of 1.4TeV $\mu^{\mp}$ composition (blue curve) together with the 1.4TeV $e^{\mp}$ peak-like contribution (green curve), in addition to the pure backgrounds (fitted by the black curve).

than the electron events in the 1.4TeV peak bin. Adding the muon decay spectrum to the background, $\Phi_e \equiv \Phi_{\mathrm{bkg}} + \Phi_{\mu \to e}$, we fit the background black points plus the red points in the non-peak-like excess region and obtain $(1.4\,\mathrm{TeV})^3 \Phi_{\mu \to e} = 883$. Thus, we deduce the ratio of event numbers between the decayed muons (N_μ) and the peak electrons (N_e), $y \equiv N_\mu / N_e \simeq 12.7$. We present our new fit of including the muon decay contribution as red dashed curve in Fig. 2(b). Impressively, it demonstrates that including the muon decay events can fully explain this non-peak-like new excess in the $(0.616 - 1.07)$TeV energy region.

4. Origin of the Flavor Structure for the CRE Excesses at DAMPE

When cosmic-ray electrons/positrons (CRE) travel across the interstellar space, they would experience diffusion due to the inverse Compton scattering. This process can be described by the following diffusion equation,

$$\frac{\partial \Phi_e}{\partial t} - \frac{\partial [b(E)\Phi_e]}{\partial E} - D(E) \bigtriangledown^2 \Phi_e = Q, \qquad (4)$$

where $\Phi_e(E_e, t, \mathbf{x})$ is a function of the $e^{\pm}$ energy and the spacetime coordinates. The energy loss, $b(E) \equiv -dE/dt$, can be parametrized as $b(E) = b_0(E/\mathrm{GeV})^2$ with $b_0 = 10^{-16}$GeV/s. The diffusion coefficient is $D(E) = D_0(E/\mathrm{GeV})^\delta$, where $D_0 = 11\mathrm{pc}^2/\mathrm{kyr}$ and $\delta = 0.7$. The right-hand-side of the above Eq.(4) is the

$e^{\pm}$ source function, $Q(\mathbf{x}, E_e) \propto \rho_\chi(\mathbf{x}) \frac{dN}{dE_e}$, where $\rho_\chi(\mathbf{x})$ is the DM density distribution and dN/dE_e is the $e^{\pm}$ energy spectrum from the DM annihilation or decay. Our calculation takes the spherically symmetric NFW density profile [18] $\rho_\chi(r) \equiv \rho_s(r/r_s)^{-\gamma}(1+r/r_s)^{\gamma-3}$ for a nearby DM subhalo.

The diffusion function (4) can be solved with Green function [19],

$$G(\mathbf{x}, E; \mathbf{x}_s, E_s) = \frac{\exp\left[-|\mathbf{x} - \mathbf{x}_s|^2/\lambda^2\right]}{b(E)(\pi\lambda^2)^{3/2}}, \qquad (5)$$

where E_s is the electron/positron energy at source and E the counterpart after diffusion. The propagation scale λ is given by $\lambda^2 = 4 \int_E^{E_s} dE' \frac{D(E')}{b(E')}$. Then, the solution of (4) can be expressed as

$$\Phi_e(E_e) = \int d^3 x_s \int dE_s G(\mathbf{x}, E_e; \mathbf{x}_s, E_s) Q(\mathbf{x}_s, E_s). \quad (6)$$

To explain the narrow peak at 1.4 TeV, the diffusion effect cannot be large. This can be achieved if the DM subhalo is close to the earth. For illustration, we choose $\gamma = 0.5$, the subhalo radius $r_s = 0.1$, and the subhalo distance $d_s = 0.2$ kpc. Consequently, the mono-energetic electron/position peak at 1.4 TeV slightly spreads to lower energy, which we show by the blue solid curve in Fig. 3. As we mentioned earlier in Sec. 3, the 1.4 TeV $\mu^{\pm}$ events have a lifetime about

0.026s, so they will decay into $e^{\pm}$ shortly after their production at the source. We have further considered the diffusion effect for the muon decay contribution. This is included in the red dashed curve in Fig. 2(b) and Fig. 3. We note that the distribution of $E_e^3 \Phi_{\mu \to e}$ in Fig. 2(a) is slightly shifted to lower energy.

From the analysis in Fig. 2 and Fig. 3, we find that the original lepton final state produced at a nearby source should have the flavor composition ratio, $N_e : (N_\mu + \frac{1}{6} N_\tau) \approx 1 : 12.7$. Note that the τ component could only play a minor role here due the suppression factor $\sim \frac{1}{6}$ by its small decay branching fraction of $\tau \to e\, \bar{\nu}_e \nu_\tau$. A simplest realization of this flavor composition condition is $N_e : N_\mu : N_\tau \approx 1 : 12.7 : 0$.

The above flavor composition condition will place important constraint on the lepton-related DM model buildings. For instance, for the typical lepton portal dark DM models [10][20], the DM is a neutral singlet (Dirac or Majorana) fermion χ and couples to a scalar mediator S and the right-handed charged lepton ℓ_{Rj}, with $\ell_j = e, \mu, \tau$,

$$\mathcal{L}_\chi \supset \lambda_j S \overline{\chi_L} \ell_{Rj} + \text{h.c.} \qquad (7)$$

Then, the DM annihilation $\chi\bar{\chi} \to \ell_j \ell_j$ goes through the t-channel exchange of S. Its annihilation cross section is proportional to λ_j^4. Thus, our simplest realization of the flavor composition condition gives $N_e : N_\mu : N_\tau = \lambda_e^4 : \lambda_\mu^4 : \lambda_\tau^4 \approx 1 : 12.7 : 0$, which means that the DM coupling to τ leptons is forbidden. So it requires a simple coupling relation, $\lambda_e : \lambda_\mu : \lambda_\tau \approx 1 : 1.9 : 0$. More generally, we have the following coupling condition,

$$\lambda_e : \left(\lambda_\mu + \frac{1}{6}\lambda_\tau\right)^{\frac{1}{4}} \approx 1 : 1.9. \qquad (8)$$

If a $\mu - \tau$ flavor symmetry requires $\lambda_\mu = \lambda_\tau$, then we find that Eq.(8) further leads to a simple coupling constraint, $\lambda_e : \lambda_\mu : \lambda_\tau \approx 1 : 1.8 : 1.8$.

Similar discussions apply to the other type of scalar DM models [10], where DM particle X is a neutral complex singlet scalar and the mediator ψ is a Dirac fermion with the same electric charge and lepton number as the charged leptons. The Lagrangian contains the relevant interaction vertex $\lambda_j X \overline{\psi_L} \ell_{Rj} + \text{h.c.}$ This also generates the t-channel DM annihilation cross section proportional to λ_j^4 and thus we can derive the same constraint from our above lepton flavor composition condition on $N_e : (N_\mu + \frac{1}{6} N_\tau)$. Further applications to the DM model buildings are encouraging and will be pursued elsewhere.

5. Conclusions

The new announcement of detecting the TeV cosmic-ray electrons/positrons (CRE) by the DAMPE collaboration [9] has brought up further excitements for probing the nearby galactic sources and possible dark matter (DM) annihilations.

In Sec. 2 of this work, we carefully inspected the DAMPE CRE energy spectrum [9] and identified a new excess of non-peak-like structure in a fairly wide region of $(0.6 - 1.1)$TeV, as shown by the red data points of Fig. 1. In Sec. 3, we conjectured that this new excess and the 1.4TeV peak excess are interconnected to each other, in the sense that they could arise from the 1.4TeV $\mu^{\pm}$ events and the 1.4TeV $e^{\pm}$ events produced together in the original galactic source at the same time (with the subsequent $\mu^{\pm}$ decays into $e^{\pm}$ plus neutrinos). We analyzed the $e^{\pm}$ energy distributions from both muon and tau decays. We found that muon decays always give the dominant contribution, as shown in Fig. 2(a). Then, we included the muon decay contribution into the fit of the DAMPE CRE spectrum, and demonstrated that this can fully explain the new excess over the $(0.6 - 1.1)$TeV energy region, as we showed in Fig. 2(b).

In Sec.4, we further performed a combined fit to the DAMPE CRE spectrum by including both the decay contribution from the 1.4TeV $\mu^{\pm}$ events and the peak contribution from the 1.4TeV $e^{\pm}$ events. For illustration, we included the diffusion effects on the CRE spectrum after the produced $e^{\pm}$ events propagate from a nearby source at a distance of about 0.2kpc to the DAMPE detector. We presented our fit to the full CRE spectrum including the decay and peak contributions together in Fig. 3. This impressively gives both the non-peak-like new excess in the $(0.6 - 1.1)$TeV region and the 1.4TeV peak excess.

Our analysis demonstrated that the *flavor structure* of the original lepton final-state produced by the DM annihilations (or other mechanism) in a nearby clump or subhalo should have a flavor composition ratio $N_e : (N_\mu + \frac{1}{6} N_\tau) \approx 1 : 12.7$. We pointed out the simplest realization, $N_e : N_\mu : N_\tau \approx 1 : 12.7 : 0$. We see that a possible τ component in the original source could only play a minor role for the observed CRE data. If the DAMPE excesses indeed arise from the DM annihilations, our study further provides important constraint on the lepton-flavor-related DM model buildings.

---

[1] P. Meyer, Annu. Rev. Astron. Astrophys. 7 (1969) 1; C. S. Shen, Astrophys. J. 162 (1970) L181; T. Kobayashi, Y. Komori, K. Yoshida, and J. Nishimura, Astrophys. J. 601 (2004) 340; Y. Z. Fan, B. Zhang, and J. Chang, Int. J. Mod. Phys. D 19 (2010) 2011.

[2] M. Turner and F. Wilczek, Phys. Rev. D 42 (1990) 1001; G. Bertone, D. Hooper, and J. Silk, Phys. Rept. 405 (2005) 279; J. L. Feng, Annu. Rev. Astron. Astrophys. 48 (2010) 495.

[3] F. Aharonian *et al.* [HESS Collaboration], Phys. Rev. Lett. 101 (2008) 261104; Astron. Astrophys. 508 (2009) 561. P. Brun [HESS Collaboration], Nucl. Part. Phys. Proc. 291-293 (2017) 25.

[4] J. Holder [for VERITAS Collaboration], AIP Conf. Proc. 1792 (2017) 020013 [arXiv:1609.02881 [astro-ph.HE]]; D. Staszak [for VERITAS Collaboration], PoS ICRC2015 (2016) 411 [arXiv:1508.06597 [astro-ph.HE]].

[5] L. Accardo *et al.* [AMS Collaboration], Phys. Rev. Lett. 113 (2014) 121101; M. Aguilar *et al.* [AMS Collaboration], Phys. Rev. Lett. 113 (2014) 121102; M. Aguilar *et al.* [AMS Collaboration], Phys. Rev. Lett. 113 (2014) 221102.

[6] S. Abdollahi *et al.* [Fermi-LAT Collaboration], Phys. Rev. D 95 (2017) 082007 [arXiv:1704.07195 [astro-ph.HE]]; M. Meehan *et al.* [Fermi-LAT Collaboration], arXiv:1708.07796 [astro-ph.HE].

[7] O. Adriani *et al.* [CALET Collaboration] Phys. Rev. Lett. 119 (2017) 181101.

[8] J. Chang *et al.,* [DAMPE Collaboration], Astroparticle Phys 95 (2017) 6 [arXiv:1706.08453 [astro-ph.IM]].

[9] G. Ambrosi *et al.,* [DAMPE Collaboration], "Direct detection of a break in the teraelectronvolt cosmic-ray spectrum of electrons and positrons", Nature (2017), in press, DOI:10.1038/nature24475 [arXiv:1711.10981 [astro-ph.HE]].

[10] Q. Yuan *et al.,* "Interpretations of the DAMPE electron data", arXiv:1711.10989 [astro-ph.HE].

[11] K. Fang, X. J. Bi, and P. F. Yin, [arXiv:1711.10996 [astro-ph.HE]].

[12] X. J. Huang, Y. L. Wu, W. H. Zhang, and Y. F. Zhou, arXiv:1712.00005 [astro-ph.HE].

[13] H. B. Jin, B. Yue, X. Zhang, X. Chen, e-Print: arXiv:1712.00362 [astro-ph.HE].

[14] F. Yang and M. Su, arXiv:1712.01724 [astro-ph.HE].

[15] Y. Z. Fan, W. C. Huang, M. Spinrath, Y. L. S. Tsai and Q. Yuan, arXiv:1711.10995 [hep-ph]; P. H. Gu and X. G. He, arXiv:1711.11000 [hep-ph]; Y. L. Tang, L. Wu, M. Zhang, R. Zheng, arXiv:1711.11058 [hep-ph]; W. Chao and Q. Yuan, arXiv:1711.11182 [hep-ph]; P. Athron, C. Balazs, A. Fowlie, and Y. Zhang, arXiv:1711.11376 [hep-ph]; J. Cao, L. Feng, X. Guo, L. Shang, F. Wang and P. Wu, arXiv:1711.11452 [hep-ph]; X. Liu and Z. Liu, arXiv:1711.11579; G. H. Duan, X. G. He, L. Wu and J. M. Yang, arXiv:1711.11563 [hep-ph]. J. S. Niu, T. Li, R. Ding, B. Zhu, H. F. Xue and Y. Wang, arXiv:1712.00372 [astro-ph.HE]; W. Chao, H. K. Guo, H. L. Li and J. Shu, [arXiv:1712.00037 [hep-ph]]; C. H. Chen, C. W. Chiang and T. Nomura, [arXiv:1712.00793 [hep-ph]]; T. Li, N. Okada and Q. Shafi, [arXiv:1712.00869 [hep-ph]]; R. Zhu and Y. Zhang, [arXiv:1712.01143 [hep-ph]]; T. Nomura and H. Okada, [arXiv:1712.00941 [hep-ph]]; K. Ghorbani and P. H. Ghorbani, [arXiv:1712.01239 [hep-ph]]; J. Cao, L. Feng, X. Guo, L. Shang, F. Wang, P. Wu, and L. Zu, arXiv:1712.01244 [hep-ph]; R. Ding, Z. L. Han, L. Feng and B. Zhu, [arXiv:1712.02021 [hep-ph]].

[16] E.g., Y. Z. Fan, W. C. Huang, M. Spinrath, Y. L. S. Tsai and Q. Yuan, [arXiv:1711.10995 [hep-ph]].

[17] K. A. Olive *et al.,* (Particle Data Group), Chin. Phys. C 40 (2016) 100001.

[18] J. F. Navarro, C. S. Frenk, and S. D. M. White, Astrophys. J. 490 (1997) 493 [arXiv:astro-ph/9611107].

[19] M. Kuhlen and D. Malyshev, Phys. Rev. D 79 (2009) 123517 [arXiv:0904.3378]; T. Delahaye, J. Lavalle, R. Lineros, F. Donato, and N. Fornengo, Astron. Astrophys. 524 (2010) A51 [arXiv:1002.1910 [astro-ph.HE]].

[20] Y. Bai and J. Berger, JHEP 1408 (2014) 153 [arXiv:1402.6696].